IOPscience iopscience.iop.org

Home Search Collections Journals About Contact us My IOPscience

Critical correlations in an ultra-cold Bose gas revealed by means of a temporal Talbot–Lau interferometer

This content has been downloaded from IOPscience. Please scroll down to see the full text.

2013 Laser Phys. Lett. 10 125502

(http://iopscience.iop.org/1612-202X/10/12/125502)

View the table of contents for this issue, or go to the journal homepage for more

Download details:

IP Address: 130.49.198.5
This content was downloaded on 08/11/2013 at 04:07

Please note that terms and conditions apply.

IOP PUBLISHING LASER PHYSICS LETTERS
Laser Phys. Lett. **10** (2013) 125502 (5pp) doi:10.1088/1612-2011/10/12/125502

LETTER

Critical correlations in an ultra-cold Bose gas revealed by means of a temporal Talbot–Lau interferometer

Wei Xiong[1], Xiaoji Zhou[1], Xuguang Yue[1], Xuzong Chen[1], Biao Wu[2,3] and Hongwei Xiong[4,5]

[1] School of Electronics Engineering and Computer Science, Peking University, Beijing 100871, People's Republic of China
[2] International Center for Quantum Materials, Peking University, Beijing 100871, People's Republic of China
[3] Collaborative Innovation Center of Quantum Matter, Beijing, People's Republic of China
[4] State Key Laboratory of Magnetic Resonance and Atomic and Molecular Physics, Wuhan Institute of Physics and Mathematics, Chinese Academy of Sciences, Wuhan 430071, People's Republic of China
[5] Department of Applied Physics, Zhejiang University of Technology, Hangzhou 310023, People's Republic of China

E-mail: xjzhou@pku.edu.cn and xionghw@zjut.edu.cn

Received 8 October 2013
Accepted for publication 14 October 2013
Published 7 November 2013
Online at stacks.iop.org/LPL/10/125502

Abstract
The transition from a thermal cloud to a Bose–Einstein condensate (BEC) in an interacting ultra-cold Bose gas is a prototype in a universality class of diverse phase transitions. For a trapped ultra-cold Bose gas, we were able to study the critical regime both above and below the critical temperature with a Talbot–Lau interferometer, observing a peak in the correlation length. From this peak, we managed to determine the universal critical exponents for this phase transition as well as the finite-size and interaction corrections to the critical temperature. The results are all in quantitative agreement with theory. This work demonstrates the potential application of the Talbot–Lau interferometer to a wide range of critical phase transitions in ultra-cold atomic gases.

S Online supplementary data available from stacks.iop.org/LPL/10/125502/mmedia

1. Introduction

Near the second-order phase transition [1–3] from a normal fluid to a superfluid characterized by a complex order parameter, the diverging spatial correlation length around the critical temperature is the driving force behind various critical phenomena. There has been enormous experimental effort to study the critical phase transition to superfluid in liquid helium [4–6]. One of the endeavors was even carried out in space to get rid of the deviation caused by gravity [7]. Many critical phenomena, which had long eluded direct experimental study, have now been studied experimentally with ultra-cold Bose [8–11] and Fermi gases [12]. Recently, there have also been intensive theoretical studies on the critical behavior with cold atoms [13–18].

The second-order phase transition from a normal state to a superfluid state has been studied in a landmark experiment [19], where the critical behavior in the correlation length was revealed by detecting the interference of two released atom beams. However, this study was limited to only the critical regime above T_c. In this work, we explore the spatial correlation with a different interference technique,

 © 2013 Astro Ltd Printed in the UK & the USA

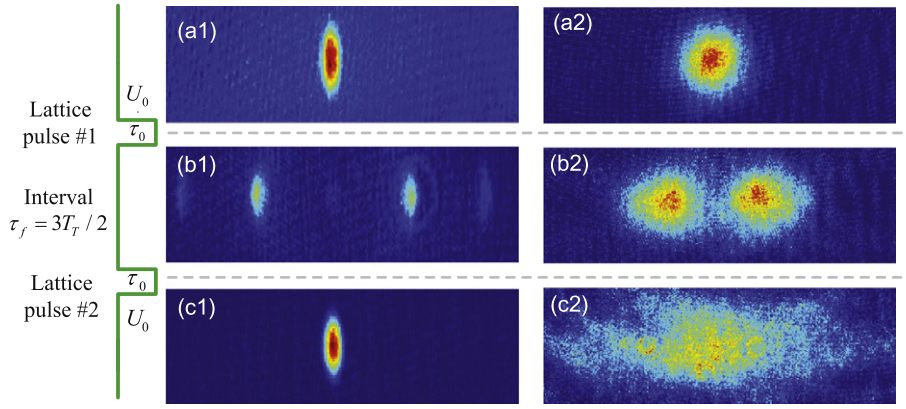

Figure 1. Effects on a pure condensate and a thermal gas by the Talbot–Lau interferometer, where two optical lattice pulses are separated by an interval τ_f equal to the odd times of half a Talbot time. The two-dimensional experimental TOF images are for (a1) a pure condensate and (a2) a thermal gas before the first lattice pulse; the momentum distributions of (b1) a BEC and (b2) a thermal gas after the first pulse; and the momentum distributions of (c1) a BEC and (c2) a thermal gas after the second pulse.

the temporal Talbot–Lau (TL) interferometer. In such an interferometer, the interference effect is greatly enhanced because all correlated atoms are manipulated rather than the two released atomic beams in [19], offering the possibility to observe the critical behavior for the spatial correlation on both sides of the critical temperature.

With this TL interferometer, we explore how the spatial correlation in an ultra-cold atomic gas varies as it undergoes the phase transition from a thermal gas to a Bose–Einstein condensate (BEC). At the critical temperature, we observe a bi-modal density distribution after the application of the TL interferometer. When the fraction of the narrower density distribution is measured, we find a clear peak in the critical regime and the peak position agrees well with the critical temperature calculated for this Bose gas by including the finite-size and interaction effects. We have also extracted the critical exponents from the measured peak and they are very close to the theoretical critical exponents for the correlation length, suggesting that the fraction measured in our experiment is proportional to the correlation length.

2. The temporal TL interferometer for ultra-cold atoms

The TL interferometer has been widely used to reveal the interference properties of different systems [20]. Here we use a temporal TL interferometer [21, 22] to experimentally study the phase transition to a BEC. Our TL interferometer (figure 1) consists of two optical lattice pulses separated by a time interval τ_f equal to the odd times of half a Talbot time $T_T = m\lambda^2/2h$ [21, 22], with λ being the laser wavelength, m the atomic mass and h Planck's constant. In our experiment, the wavelength $\lambda = 852$ nm, the interval $\tau_f = 3T_T/2$, the pulse width $\tau_0 = 3$ μs, and the lattice depth $U_0 = 80E_R$, with E_R being the recoil energy of an atom absorbing one lattice photon. The lattice depth is calibrated experimentally by the Kapitza–Dirac scattering. The ultra-cold atoms of ^{87}Rb were prepared in a magnetic trap with an axial frequency of 20 Hz and a radial frequency of 220 Hz [23]. The TL interferometer was applied to the ultra-cold atomic gas along the axial direction. The time-of-flight (TOF) images were obtained with the standard absorption imaging method after switching off the magnetic field and 30 ms free expansion.

During the first lattice pulse, the atomic gas is divided into hundreds of disk-shaped atomic gases that are physically separated due to the strength of the pulse. After the pulse, these disk-shaped atomic gases start to merge and interfere for a given time. The second lattice pulse again divides the atomic gas into hundreds of disk-shaped atomic gases, leading to a second interference. For an initial atomic gas without correlation, the interference is in fact for each individual atom itself. The overall interference pattern is a simple addition of the interference intensities for all the individual atoms in the gas. Such a simple addition does not apply for an atomic gas with spatial correlation larger than the spatial period of the pulsed lattice. Due to the correlation, one should instead sum up first the interference wavefunctions for the correlated atoms within the correlation length, then square the amplitude of the summed wavefunction to obtain an enhanced interference. This enhancement suggests that the TL interferometer would be powerful for the detection of the spatial correlation among atoms.

Our TL interferometer is effectively an interferometer for atoms around zero momentum and with spatial correlation larger than the spatial period of the pulsed optical lattices. To clearly see this, we turn to the momentum space, where the experimental observation is made, and focus on atoms with momenta very close to zero. For these atoms, after the first optical lattice pulse, a significant proportion of the atoms will be transferred to momenta around $\pm 2n\hbar k$ ($k = 2\pi/\lambda$, $n = 1, 2, 3, \ldots$) with almost no atoms left at zero momentum; after the second optical lattice pulse, the atoms with momenta around $\pm 2n\hbar k$ will be brought back to momenta around $0\hbar k$ [24]. This effect is verified and illustrated experimentally with a pure condensate in the left column of figure 1.

With this in mind, it is straightforward to see how our interferometer will affect a thermal atomic cloud without correlation: a very small fraction of atoms that are in states of

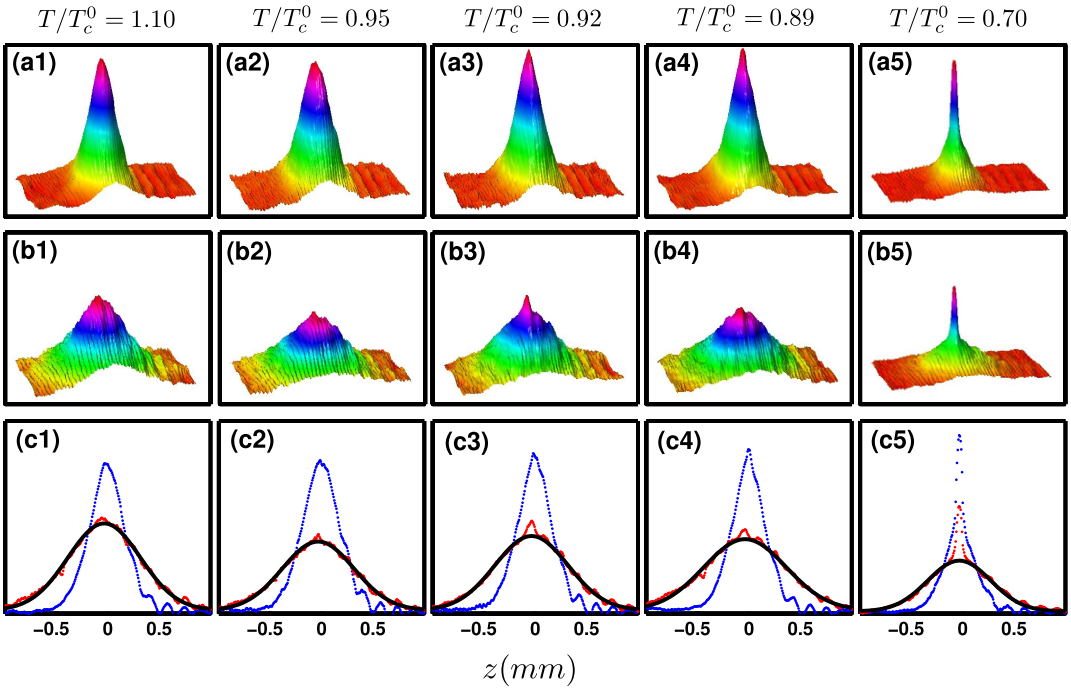

Figure 2. Revelation of the critical phase transition from a thermal cloud to a BEC by the TL interferometer. The first row shows the density distributions of the atomic gases before the TL interferometer for five different temperatures $T/T_c^0 = 1.10, 0.95, 0.92, 0.89, 0.70$. The density distributions after the TL interferometer are shown in the second row. The dotted blue lines and dotted red lines in (c1)–(c5) give the one-dimensional density distributions after the integration of the two-dimensional density distributions along the vertical direction for (a1)–(a5) and (b1)–(b5), respectively. A bi-modal structure emerges after the TL pulses in (b3) and reveals the critical phase transition occurring around $T/T_c^0 = 0.92$. In (c1)–(c5), the solid black lines give the Gaussian fitting to the broad peak of the density distribution after the TL interferometer.

momentum zero are similarly transferred away and brought back to momentum zero by our interferometer; for the majority of the atoms with non-zero momenta, they will not be brought back to their original momentum states. The end result is an atomic cloud with a much wider distribution in momentum space (see the right column of figure 1). For the thermal atomic cloud, because of the lack of correlation between different momentum states, it is expected that there is a trivial mapping before and after the TL interferometer. Both experiment and theoretical simulation show that the momentum distribution is still a Gaussian distribution after the TL interferometer.

Far below the critical temperature which comprises both condensate and thermal atoms, after the application of the TL interferometer, we expect a bi-modal density distribution because the condensate will still lead to a narrower central peak, as experimentally shown in figure 2(b5).

When the system is close to the critical temperature, there is strong spatial correlation between atoms, which will enhance the interference, as reported in [19]. As our TL interferometer is essentially an interferometer for atoms around momentum zero, this enhancement is expected to increase the population around momentum zero, causing the momentum distribution around zero to deviate from the Gaussian distribution after the application of the TL interferometer. Such a deviation from the Gaussian should be larger for stronger correlation. In a sense, the existence of an order parameter for the correlated atoms within the critical regime makes these atoms have similar behavior to a condensate after the application of the TL interferometer. This physical picture will lead to a bi-modal density distribution after the application of the TL interferometer, similarly to the system far below the critical temperature.

Within the critical regime marked by the Ginzburg temperature T_G, i.e. $|T - T_c| < T_G$, the correlation length diverges near the critical temperature T_c as [1–3]

$$\xi = \xi_0/(T - T_c)^{\nu} \qquad \text{for } T > T_c, \tag{1}$$

$$\xi_T = \xi_0^T/(T_c - T)^{\nu_T} \qquad \text{for } T < T_c, \tag{2}$$

where the critical exponents $\nu = \nu_T = 0.67$. This is for the infinite system in the thermodynamic limit. For the finite system in our experiment, the correlation length no longer diverges. Nevertheless, the correlation is still strongest at the critical temperature T_c and the correlation length should have a peak around T_c. Within the critical regime, this implies that the deviation from the Gaussian distribution after the TL interferometer is largest at T_c.

3. Observation of the critical phase transition

With the above expectations, we have surveyed the ultra-cold atomic gases with the TL interferometer over a wide range of temperatures with particular attention paid to the range where the critical phase transition from a thermal cloud to a BEC occurs. The results for five typical temperatures are

shown in figure 2. The system temperature is expressed in terms of $T_c^0 = 0.94\hbar\omega_{ho}N^{1/3}/k_B$, the critical temperature of the corresponding ideal Bose gas without the finite-size correction [25]. $\omega_{ho} = (\omega_x\omega_y\omega_z)^{1/3}$ is the geometric average of the harmonic trapping frequencies and N is the total particle number.

The first row of the figure shows TOF images before the application of the TL interferometer. The corresponding integrated density distributions are shown as dotted blue lines in the third row. There is a clear bi-modal distribution at temperature $T/T_c^0 = 0.7$ (figure 2(a5)) and a minor bi-modal distribution at temperature $T/T_c^0 = 0.89$ (figure 2(a4)). There is no obvious condensate fraction at three other higher temperatures. However, after the application of the TL interferometer, a clear bi-modal (i.e., non-Gaussian) distribution emerges at $T/T_c^0 = 0.92$ (figure 2(b3)). In contrast, at a temperature well above the critical temperature ($T/T_c^0 = 1.1$), and temperatures ($T/T_c^0 = 0.89$) and ($T/T_c^0 = 0.95$), there are no obvious bi-modal structures after the application of the TL interferometer. This shows that the emergence of the bi-modal distribution at $T/T_c^0 = 0.92$ is the result of the diverging correlation length near the critical temperature.

To quantify the observed critical behavior, we use the fraction of atoms in the central peak of the bi-modal structure after the TL pulses for different temperatures. For each density distribution obtained after the TL interferometer, we fit it along the direction of the TL pulses with a bi-Gaussian function, and compute the fraction of the central narrow peak with $f_r = 1 - A_b/A_T$, where A_b is the area under the broad peak and A_T is the total area in the bi-modal structure. Note that it is an assumption that the non-Gaussian distribution of momentum observed near T_c is bi-modal. This assumption is reasonable, as indicated in figure 2(b3) (see the supplementary material (available at stacks.iop.org/LPL/10/125502/mmedia) for further discussion).

In figure 3, we show how this fraction f_r changes with temperature. Near the critical temperature, a clear peak around $T/T_c^0 = 0.92$ is seen. We also notice a small dip in the peak, which may due to the uncertainty in the temperature calibration which is about $0.01T_c^0$. Because the central peak after the TL interferometer physically originates from the spatial interference of the atoms, within the critical regime, it is expected that the larger the correlation length, the larger the fraction f_r. Hence, this peak implies the critical phase transition from a thermal cloud to a BEC.

As the correlation length diverges at the critical temperature, this peak position can be regarded as the critical temperature of the system. Above this critical temperature, the fraction f_r increases with decreasing temperature, very similarly to what was observed with the method of matter–wave interference [19]. Below this critical temperature, we see that f_r decreases with decreasing system temperature within the critical regime.

From the peak in figure 3, we are able to determine the critical temperature T_c. We find $T_c/T_c^0 = 0.92 \pm 0.01$, indicating a negative shift from the critical temperature T_c^0 of the ideal Bose gas. The negative shift is due to

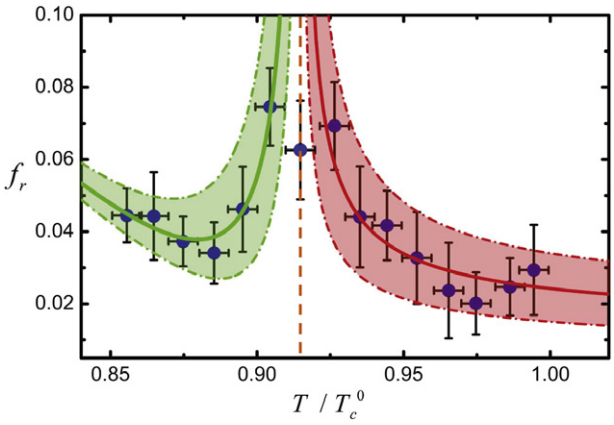

Figure 3. The measured fraction f_r of the central peak as a function of temperature. Each point is an average over about ten experimental data within a temperature step $\delta T/T_c^0 = 0.01$. The two solid lines are fittings to the data near the peak with equations (1) and (2). The colored areas represent the uncertainties with a 95% confidence. The vertical dashed line shows the location of the theoretical critical temperature.

the finite-size and interaction corrections of the critical temperature. Simultaneous consideration of the finite-size and interaction corrections to the critical temperature [26, 27] gives a negative shift of about 0.08, agreeing well with our experimental result $T_c/T_c^0 = 0.92 \pm 0.01$. The correction to the critical temperature also agrees with previous experiments [29–32]. These agreements further confirm the observation of the critical phase transition in this work. It is worth pointing out that we have computed the Ginzburg temperature T_G/T_c^0 [26]. The result is that $|T_G - T_c|/T_c^0 \approx 0.06$, which agrees with the peak width in figure 3.

Below the critical temperature and within the critical regime, there is a decrease of f_r. This is because the fraction f_r has two origins, the condensate fraction that has perfect coherence and the correlated thermal fraction that obeys equation (2). Within the critical regime, the contribution from the correlated thermal fraction dominates, causing the fraction f_r to decrease. In fact, we measured the condensate fraction without the TL interferometer. The results agree with the theoretical result by taking into account the finite-size and interaction corrections [26–28]. At $T = 0.85T_c^0$, just outside the critical regime and where the fraction starts to increase, our experiment shows that the condensate fraction without the interferometer is about 0.08, which is of the order of f_r in figure 3. We emphasize that this understanding of the whole system consisting of two parts, condensate and correlated thermal atoms, is phenomenological in the spirit of the two-fluid model for liquid helium. A more rigorous theory is needed to fully understand the strongly correlated quantum many-body state just below the critical temperature and how it responds to an interferometer.

4. Discussion and outlook

Within the critical regime, it is clear that the fraction f_r is a monotonic function of the correlation length. It is natural

to fit the data on the right side of the peak with $a/(T/T_c^0 - T_c/T_c^0)^{\tilde{\nu}} + b$ and the left side with $a'/(T_c/T_c^0 - T/T_c^0)^{\tilde{\nu}'} + b' + c'(T_c/T_c^0 - T/T_c^0)$. The additional term for the left side is to account for the condensate fraction which appears below the critical temperature. Rigorously speaking, the correlation length should display a smooth evolution within the critical regime due to the finite-size characteristic of our experiment. Similarly to [19], because of the uncertainty in the temperature calibration, we do not discuss the finite-size effect on the correlation length in this work.

From the data fitting, we get $\tilde{\nu}' = 0.70 \pm 0.08$ and $\tilde{\nu} = 0.70 \pm 0.11$. The uncertainties correspond to a 95% confidence level. These two critical exponents are very close to $\nu = \nu_T = 0.67$, the theoretical value of the correlation length's critical exponent for the universality class of the three-dimensional XY model [33, 34]. If we assume that $f_r \sim \xi^{\alpha}$ and the theoretical value of the critical exponent is exact, we have $\alpha \approx 1.04 \pm 0.12$. This experimental result indicates that the fraction f_r near the peak in figure 3 is proportional to the correlation length.

This encouraging indication is supported by a phenomenological theory (see the supplementary material available at stacks.iop.org/LPL/10/125502/mmedia). However, we still do not have a rigorous theory of how a strongly correlated system responds to an interferometer, as the action of the interferometer can no longer be regarded as a small perturbation. This is different from known measurements on critical systems, for example, heat capacity measurements on liquid helium, which can be regarded as perturbations and have negligible effects on the systems.

In summary, we have studied the critical behavior of interacting ultra-cold Bose gases with a temporal TL interferometer. A peak in the fraction of the narrower peak of the density distribution was clearly observed across the phase transition from a thermal gas to a BEC. This observation of the peak is a direct revelation of the diverging correlation length around the critical temperature, as the critical temperature obtained from this lambda peak agrees with the theoretical prediction. This experimental study of ultra-cold atomic gas within the critical regime opens a route to relevant theoretical studies of critical dynamics, which has many open problems [1–3]. It also gives a new method to measure the critical temperature. We anticipate that the temporal TL interferometer will be used to study a wide range of critical phase transitions, such as the quantum phase transition from superfluid to Mott insulator for cold atoms in an optical lattice [8], ultra-cold Fermi gas [12] and quantum magnetism with cold atoms and molecules as a quantum simulator [9, 35–37].

Acknowledgments

This work was supported by the NBRP of China (2011CB921500, 2012CB921300), the NSF of China (61078026, 11175246, 10825417, 11334001), and the RFDP of China (20110001110091). We thank W Vincent Liu, Cheng Chin, Hui Zhai for useful discussions.

References

[1] Zinn-Justin J 2002 *Quantum Field Theory and Critical Phenomena* (Oxford: Oxford University Press)
[2] Chaikin P M and Lubensky T C 2000 *Principles of Condensed Matter Physics* (Cambridge: Cambridge University Press)
[3] Privman V, Hohenberg P C and Aharony A 1991 *Phase Transitions and Critical Phenomena* vol 14, ed C Domb and J L Lebowitz (New York: Academic)
[4] Greywall D and Ahlers G 1973 *Phys. Rev.* A **7** 2145
[5] Ahlers G 1973 *Phys. Rev.* A **8** 530
[6] Adriaans M J, Swanson D R and Lipa J A 1994 *Physica* B **194** 733
[7] Lipa J A, Nissen J A, Stricker D A, Swanson D R and Chui T C P 2003 *Phys. Rev.* B **68** 174518
[8] Greiner M, Mandel O, Esslinger T, Hänsch T W and Bloch I 2002 *Nature* **415** 39
[9] Simon J, Bakr W S, Ma R, Tai M E, Preiss P M and Greiner M 2011 *Nature* **472** 307
[10] Zhang X, Hung C-L, Tung S-K and Chin C 2012 *Science* **335** 1070
[11] Hung C-L, Zhang X, Gemelke N and Chin C 2011 *Nature* **470** 236
[12] Ku M J H, Sommer A T, Cheuk L W and Zwierlein M W 2012 *Science* **335** 563
[13] Kato Y, Zhou Q, Kawashima N and Trivedi N 2008 *Nature Phys.* **4** 617
[14] Campostrini M and Vicari E 2009 *Phys. Rev. Lett.* **102** 240601
[15] Zhou Q and Ho T-L 2010 *Phys. Rev. Lett.* **105** 245702
[16] Diehl S, Baranov M, Daley A J and Zoller P 2010 *Phys. Rev. Lett.* **104** 165301
[17] Hazzard K R A and Mueller E J 2011 *Phys. Rev.* A **84** 013604
[18] Fang S, Chung C-M, Ma P N, Chen P and Wang D-W 2011 *Phys. Rev.* A **83** 031605
[19] Donner T, Ritter S, Bourdel T, Ottl A, Köhl M and Esslinger T 2007 *Science* **315** 1556
[20] Cronin A D and Pritchard D E 2009 *Rev. Mod. Phys.* **81** 1051
[21] Cahn S B, Kumarakrishnan A, Shim U, Sleator T, Berman P R and Dubetsky B 1997 *Phys. Rev. Lett.* **79** 784
[22] Deng L, Hagley E W, Denschlag J, Simsarian J E, Edwards M, Clark C W, Helmerson K, Rolston S L and Phillips W D 1999 *Phys. Rev. Lett.* **83** 5407
[23] Xiong W, Yue X, Wang Z, Zhou X and Chen X 2011 *Phys. Rev.* A **84** 043616
[24] Edwards M, Benton B, Heward J and Clark C W 2010 *Phys. Rev.* A **82** 063613
[25] Pethick C J and Smith H 2002 *Bose–Einstein Condensation in Dilute Gases* (Cambridge: Cambridge University Press)
[26] Giorgini S, Pitaevskii L P and Stringari S 1996 *Phys. Rev.* A **54** R4633
[27] Xiong H, Liu S, Huang G and Xu Z 2002 *Phys. Rev.* A **65** 033609
[28] Xiong H, Liu S, Huang G, Xu Z and Zhang C 2001 *J. Phys. B: At. Mol. Phys.* **34** 3013
[29] Ensher J R, Jin D S, Matthews M R, Wieman C E and Cornell E A 1996 *Phys. Rev. Lett.* **77** 4984
[30] Gerbier F, Thywissen J H, Richard S, Hugbart M, Bouyer P and Aspect A 2004 *Phys. Rev. Lett.* **92** 030405
[31] Smith R P, Campbell R L D, Tammuz N and Hadzibabic Z 2011 *Phys. Rev. Lett.* **106** 250403
[32] Smith R P, Tammuz N, Campbell R L D, Holzmann M and Hadzibabic Z 2011 *Phys. Rev. Lett.* **107** 190403
[33] Burovski E, Machta J, Prokof' ev N and Svistunov B 2006 *Phys. Rev.* B **74** 132502
[34] Yukalov V I and Yukalova E P 2007 *Eur. Phys. J.* B **55** 93
[35] Sachdev S 2008 *Nature Phys.* **4** 173
[36] Jo G-B, Lee Y-R, Choi J-H, Christensen C A, Kim T H, Thywissen J H, Pritchard D E and Ketterle W 2009 *Science* **325** 1521
[37] Gorshkov A V, Manmana S R, Chen G, Ye J, Demler E, Lukin M D and Rey A M 2011 *Phys. Rev. Lett.* **107** 115301